





RESEARCH ARTICLE | SEPTEMBER 04 2025

Arnold tongues replace period-doubling cascades in a memristor circuit

Silvio L. T. de Souza   ; Antonio M. Batista  ; Iberê L. Caldas 



Chaos 35, 093106 (2025)

<https://doi.org/10.1063/5.0277414>



Articles You May Be Interested In

Reverse Newhouse–Ruelle–Takens route to chaos and time-dependent Hamiltonian formulation of a generalized Muthuswamy–Chua system

Chaos (January 2026)

On the dynamics of the Muthuswamy–Chua systems in \mathbb{R}^3

Chaos (April 2025)

Chaos in electronic circuits and studies of bifurcation mechanisms

AIP Conf. Proc. (October 2013)



AIP Advances

Why Publish With Us?

-  **21DAYS**
average time to 1st decision
-  **OVER 4 MILLION**
views in the last year
-  **INCLUSIVE**
scope

[Learn More](#)



Arnold tongues replace period-doubling cascades in a memristor circuit

Cite as: Chaos 35, 093106 (2025); doi: 10.1063/5.0277414

Submitted: 23 April 2025 · Accepted: 16 August 2025 ·

Published Online: 4 September 2025






View Online



Export Citation



CrossMark

Silvio L. T. de Souza,^{1,2,a)}  Antonio M. Batista,^{3,4}  and Iberê L. Caldas² 

AFFILIATIONS

¹Federal University of São João del-Rei, Campus Centro-Oeste, 35501-296 Divinópolis, MG, Brazil

²Institute of Physics, University of São Paulo, 05508-900 São Paulo, SP, Brazil

³Graduate Program in Science, State University of Ponta Grossa, 84030-900 Ponta Grossa, PR, Brazil

⁴Department of Mathematics and Statistics, State University of Ponta Grossa, 84030-900 Ponta Grossa, PR, Brazil

^{a)}Author to whom correspondence should be addressed: thomaz@ufsj.edu.br

ABSTRACT

The memristor, theorized by Leon Chua in 1971, functions as a fundamental electronic component, directly linking electric charge and magnetic flux. As a result of their nonlinear characteristics, memristive circuits generally exhibit chaotic attractors in addition to periodicity. In this work, we consider the Muthuswamy–Chua system, a chaotic circuit consisting of an inductor, a capacitor, and a memristor. In two-dimensional parameter spaces, this system displays periodic shrimp-shaped domains, which are periodic windows surrounded by chaotic regions. Applying a weak harmonic perturbation, we observe the replacement of periodicity by quasiperiodicity, followed by the formation of Arnold tongues (periodic structures) acting as boundaries between quasiperiodic and chaotic regions. Moreover, as an additional result of the perturbation, we identify another interesting feature: the metamorphosis of quasiperiodic shrimp-shaped domains into Arnold tongues. In both instances, Arnold tongues emerge in regions previously dominated by period-doubling cascades under unperturbed conditions.

Published under an exclusive license by AIP Publishing. <https://doi.org/10.1063/5.0277414>

In circuit theory, resistor, capacitor, and inductor configure as the fundamental two-terminal circuit elements. In 1971, Professor Leon Chua proposed the memristor as the fourth basic circuit element. Together, these four elements complete the theoretical relationships between the core electrical quantities: current, voltage, charge, and magnetic flux. In 2008, after decades of the initial concept, researchers from HP lab built the first device, presenting memristance properties. The key point about the memristor is its memory-dependent resistance, i.e., its state depends on the history of the current or voltage. As a prototypal example of a memristor system, Muthuswamy and Chua proposed the simplest chaotic circuit comprised of only three elements: a capacitor, an inductor, and a memristor. This system exhibits the typical scenario of chaos involving period-doubling bifurcations. In the two-dimensional parameter space, periodic structures surrounded by chaotic regions appear as shrimp-shaped domains. In this work, we investigate the effect of a weak periodic perturbation on the Muthuswamy–Chua circuit. First, we verify the replacement of periodicity by quasiperiodicity for a tiny perturbation. By increasing perturbation, we observe the emergence

of Arnold tongues in the transition region from quasiperiodicity to chaotic domains. For shrimps, the quasiperiodic structures gradually vanish, then transition into Arnold tongues and subsequently transform the tongues into a complex and seemingly disordered distribution of periodic domains.

I. INTRODUCTION

A memristor, short for memory resistors, is a passive circuit element that was theorized by Chua in 1971¹ as the fourth fundamental circuit element, alongside the resistor, capacitor, and inductor. In 2008, Strukov *et al.*² identified the missing element, reporting a functional memristor based on a bi-level titanium dioxide thin film with dopants. Yang *et al.*³ provided experimental evidence of memristive electrical switching in oxide systems. Memristive devices can be designed and fabricated using various methods and materials.^{4,5} Furthermore, this fundamental passive electrical component has an extensive range of applications, including secure communication,⁶ reconfigurable electromagnetic devices,⁷

programmable analog circuits,⁸ artificial synapses,⁹ and experimental results demonstrating spike-timing-dependent plasticity in metal-oxide materials.¹⁰

Another relevant feature of memristors is their nonlinearity in mathematical descriptions, implying diversity and rich dynamical behaviors. For instance, the simplest chaotic circuit was proposed by Muthuswamy and Chua.¹¹ This circuit comprises a linear passive capacitor, a linear passive inductor, and a nonlinear active memristor. By varying the control parameters, the system can exhibit periodic attractors, period-doubling bifurcations, chaotic attractors, and intermittency.^{12,13} For this system, Furui and Takano,¹⁴ considering a sinusoidal perturbation, identified the intriguing phenomenon of the devil's staircase.

In nonlinear analysis, the characterization of dynamics in two-dimensional parameter space using Lyapunov exponents has been extensively explored for various systems, including parametric pendulums,¹⁵ impact oscillators,^{16,17} red grouse population models,¹⁸ predator–prey models,^{19–21} electronic circuits,²² and plasma physics,^{23,24} to name just a few. In many cases, periodic structures surrounding chaotic regions appear highly organized, exhibiting typical self-similarity associated with Arnold tongues and shrimp-shaped domains.^{25–29} These structures have generally been classified as periodic solutions.^{30–32} However, recent studies have reported substantial findings in the study of quasiperiodicity. Stankevich *et al.*³³ identified tongues and shrimp-shaped domains composed of quasiperiodic attractors in a continuous-time model of radio-physical generators. Similarly, Pati³⁴ identified quasiperiodic shrimps displaying spiral organization in a discrete-time predator–prey model. More recently, Pati *et al.*³⁵ investigated quasiperiodic shrimp organizations in a discrete-time food chain model. They highlighted a vital feature: unlike the periodic case, these structures exhibit a limited number of doubling bifurcations before reaching chaos. Along the same line, de Souza *et al.*³⁶ reported remarkable pattern formation of quasiperiodic domains in an intrinsically coupled system described by Lagrangian formalism. Besides quasiperiodic shrimps, they identified self-similar metamorphic tongues, a set of self-similar islands exhibiting an interwoven pattern of chaotic, quasiperiodic, and periodic regions.

In this work, we examine the effect of a weak harmonic perturbation on the Muthuswamy–Chua system in a two-dimensional parameter space. In addition to replacing periodicity by quasiperiodicity, we observe the emergence of Arnold tongues in two cases: as boundaries between quasiperiodic and chaotic regions, and as transformations of quasiperiodic shrimps.

This article is organized as follows: Section II provides the mathematical formulation of the Muthuswamy–Chua system with a harmonic perturbation. In Sec. III, we explore the effects of perturbation on dynamic behavior. In Sec. IV, we elaborate on the mechanism responsible for the transformation observed in the parameter space. Finally, our last remarks are presented in Sec. IV.

II. MUTHUSWAMY-CHUA SYSTEM WITH HARMONIC PERTURBATION

The mathematical formulation of the Muthuswamy–Chua system,¹¹ composed of a capacitor, an inductor and a memristive

element, with harmonic perturbation is given by¹⁴

$$\begin{aligned} \dot{x} &= \frac{y}{C}, \\ \dot{y} &= -\frac{1}{L} [x + \beta(z^2 - 1)y + \gamma \sin \omega t], \\ \dot{z} &= -y - \alpha z + \gamma z, \end{aligned} \quad (1)$$

where the dynamical variable $x(t)$ represents the voltage across the capacitor C , while $y(t)$ represents the current through the inductor L . The internal state of the memristive element is described by $z(t)$. The parameters γ and ω denote the amplitude and frequency of the sinusoidal perturbation, respectively.

III. QUASIPERIODICITY AND ARNOLD TONGUES

In this section, we present numerical results in two-parameter spaces for the Muthuswamy–Chua system with a harmonic perturbation. For our numerical analysis, we employed the fourth-order Runge–Kutta method with a fixed time step of 10^{-2} , discarding a transient phase of 2.0×10^5 iterations, and using an additional 2.0×10^7 trajectory points to compute the Lyapunov exponents. These exponents were evaluated using the Benettin algorithm,³⁷ with the code provided by Wolf and collaborators.³⁸ In addition, we consider the control parameters α , β from intrinsic characteristics of the memristor, and γ and ω from the amplitude and frequency of a perturbation term, respectively. The remaining parameters were fixed at $C = 1.2$ and $L = 3.3$, according to ones used in a physical circuit implemented by Muthuswamy and Chua.¹¹

Initially, we illustrate the representative behaviors of the memristive circuit in the absence of perturbation, $\gamma = 0$. Figure 1(a) displays a bifurcation diagram, showing the asymptotic values of the local maximum x as a function of β . To characterize the attractors, we plot the three corresponding Lyapunov exponents in Fig. 1(b), disregarding the zero exponent and focusing on the largest Lyapunov exponent: a positive value indicates a chaotic attractor, a negative value indicates a periodic attractor, and zero indicates a bifurcation in smooth systems or a quasiperiodic attractor. In Fig. 1(a), we observe only periodic and chaotic attractors, framing a route to chaos via period-doubling bifurcation, with the usual chaotic range interspersed with periodic windows.

Turning our attention to quasiperiodicity, Fig. 2(a) exhibits the bifurcation diagrams of the system under harmonic perturbation for $\gamma = 0.01$. Utilizing the previous attractors in black ($\gamma = 0$) to emphasize the transformation of the new attractors in brown, we observe that the lines representing periodic solutions are no longer present. The perturbation promotes enlargement on the dynamical variable x , especially around the period-doubling bifurcation. In Fig. 2(b), as perturbation increases for $\gamma = 0.10$, the transformation of the attractors becomes more pronounced.

In fact, a weak harmonic perturbation causes the system to evolve from a single-frequency (periodic) to a multi-frequency regime (quasiperiodic). In this case, the system incorporates a fourth Lyapunov exponent, replacing the previous three-exponent configuration. Figures 3(a)–3(d) illustrate this transformation process for the attractors, whose parameters are indicated by dashed lines in Figs. 2(a) and 2(b). Using a return mapping x_{n+1} vs x_n , Fig. 3(a)

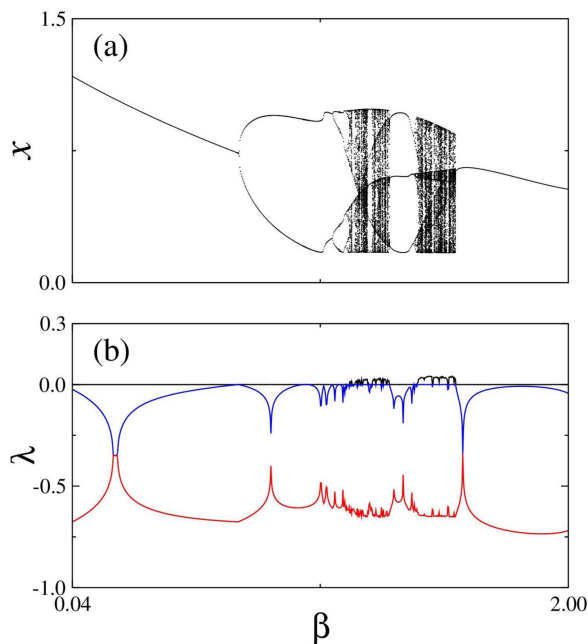


FIG. 1. (a) Bifurcation diagram of the local maxima of x as a function of β and (b) Lyapunov exponents for $C = 1.2$, $L = 3.3$, $\alpha = 0.7$, and $\gamma = 0$.

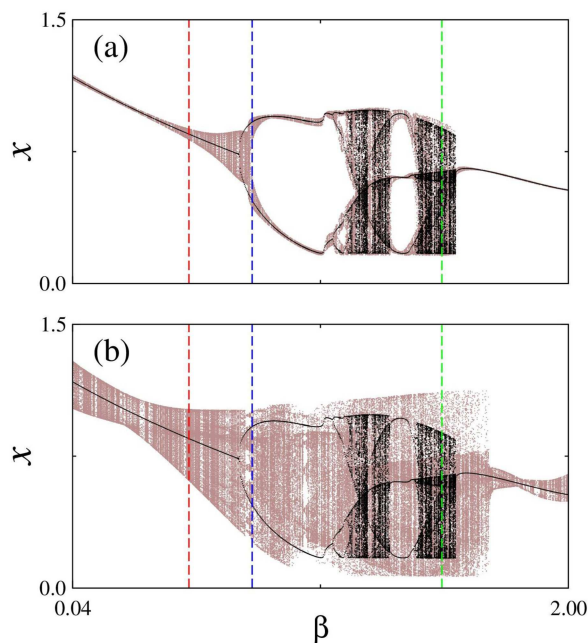


FIG. 2. Bifurcation diagram varying β for $C = 1.2$, $L = 3.3$, $\alpha = 0.7$, and $\omega = 0.28$. The background is shown in brown for (a) $\gamma = 0.01$ and (b) $\gamma = 0.1$. The diagram plotted in black is the same as in Fig. 1(a) for $\gamma = 0.0$.

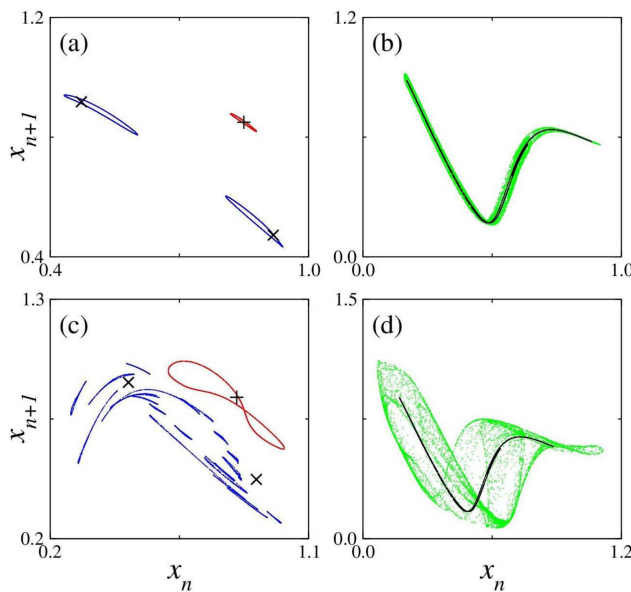


FIG. 3. Overview of the attractors: (a) A torus in red for $(\beta, \gamma) = (0.50, 0.01)$ and a torus in blue for $(\beta, \gamma) = (0.75, 0.01)$. (b) A chaos on torus in green for $(\beta, \gamma) = (1.36, 0.01)$. (c) A torus in red for $(\beta, \gamma) = (0.50, 0.10)$ and a chaotic attractor in blue for $(\beta, \gamma) = (0.75, 0.10)$. (d) A chaos on torus in green for $(\beta, \gamma) = (1.36, 0.10)$. These attractors are indicated by dashed lines in the bifurcation diagram from Figs. 2(a) and 2(b). The corresponding attractors for $\gamma = 0.0$ are plotted in black.

shows the evolution of the period-1 attractor (depicted in black with plus symbols) and the period-2 attractor (depicted in black with “x” symbols) for $\gamma = 0$ into a single-torus (in red) and a double-torus (in blue) for $\gamma = 0.01$. In Fig. 3(c), increasing perturbation to $\gamma = 0.10$, the single-torus (in red) undergoes stretching in phase space, while the double-torus becomes a chaotic attractor with bands (in blue) for the largest Lyapunov exponent $\lambda \approx 0.002$ (not shown in the figure). In Figs. 3(b) and 3(d), the chaotic attractor (in black) transforms into a chaos on torus (in green), exhibiting two zero Lyapunov exponents and one positive exponent ($\lambda \approx 0.038$). As perturbation increases from $\gamma = 0.01$ [Fig. 3(b)] to $\gamma = 0.10$ [Fig. 3(d)], the attractor (in green) expands significantly in size, exhibiting chaotic behavior characterized by a single zero exponent alongside a positive exponent ($\lambda \approx 0.026$), rather than the two zero exponents observed in chaos on the torus state.

To gain further insights into the quasiperiodic process, we evaluate the Lyapunov exponents for a two-dimensional parameter diagram for γ vs β for a grid of 800×800 cells. Varying the amplitude of perturbation from $\gamma = 0$ to $\gamma = 0.2$, Fig. 4 displays the evolution of the attractors indicated in the bifurcation diagram of Fig. 1(a). Periodic attractors are shown in black, chaotic attractors in white, and quasiperiodic attractors in blue. Due to perturbation, periodic attractors immediately transition into quasiperiodic attractors (in blue). Subsequently, periodic attractors emerge, forming the boundary of Arnold tongues (in black) between quasiperiodic and chaotic regions. These periodic tongues play an essential role in

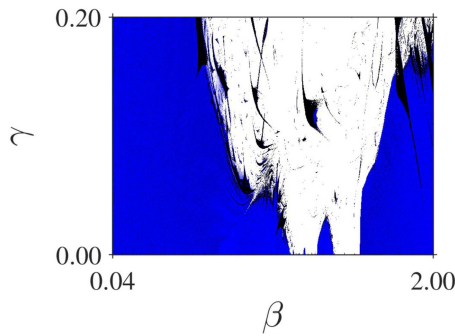


FIG. 4. Parameter plane diagram for γ vs β , showing the evolution of the attractors indicated in the bifurcation diagram of Fig. 1(a). Periodic attractors are plotted in black, chaotic attractors in white, and quasiperiodic attractors in blue. The control parameters are fixed at $C = 1.2$, $L = 3.3$, $\alpha = 0.7$, and $\omega = 0.28$.

illustrating the route to chaos from quasiperiodicity, as described in the Curry–Yorke scenario.^{39–41} Beyond the case of a weak harmonic perturbation, quasiperiodicity can also be studied under a perturbation with two incommensurate frequencies. However, in this case, the route to chaos follows a torus-doubling bifurcation scenario, which is interrupted by the emergence of strange nonchaotic attractors.^{42–45}

To examine the effect of perturbation in greater detail, Figs. 5(a)–5(d) exhibit a sequence of parameter plane diagrams for

α vs β as a function of γ . First, for $\gamma = 0$, Fig. 5(a) displays a parameter plane where periodic windows (in black) are surrounded by a chaotic region (in white). The blue lines represent period-doubling bifurcations and the periodic windows exhibit a characteristic shape known as shrimps.²⁵ For a tiny perturbation $\gamma = 0.001$ in Fig. 5(b), periodic regions become quasiperiodic (in blue). In addition, we observe the vanishing of quasiperiodic shrimps, evidenced by the green region. This green region represents chaotic attractors that were previously periodic at $\gamma = 0$. Increasing perturbation gradually in Figs. 5(c)–5(f), we verify the progression of the vanishing process in quasiperiodic shrimps and the emergence of periodic structures (in black). Surprisingly, a significant portion of the periodic domains emerges well-structured, manifesting as Arnold tongues and forming the boundaries between quasiperiodic and chaotic regions.

At first glance for the shrimps, perturbation just induces the quasiperiodicity and the vanishing process, promoting the enlargement of chaos regions. In Figs. 6(a)–6(f), we analyze the transformation of shrimps in detail. For the unperturbed case $\gamma = 0$, Fig. 6(a) shows a collection of periodic shrimps obtained from a magnification of the yellow box depicted in Fig. 5(a). For the perturbed cases from $\gamma = 0.001$ to $\gamma = 0.020$, Figs. 6(b)–6(f) illustrate the retraction of quasiperiodic shrimps and the emergence of intricate periodic structures (in black). In fact, this periodicity reveals another interesting feature. The periodic domains appear as Arnold tongues covering the upper side of the quasiperiodic shrimps, as more clearly shown in Figs. 7(a)–7(c) from $\gamma = 0.020$ to $\gamma = 0.024$. As perturbation increases, the self-similar pattern of the tongues evolves into a complex distribution of periodicity, as shown in Figs. 7(d)–7(f), from $\gamma = 0.026$ to $\gamma = 0.030$.

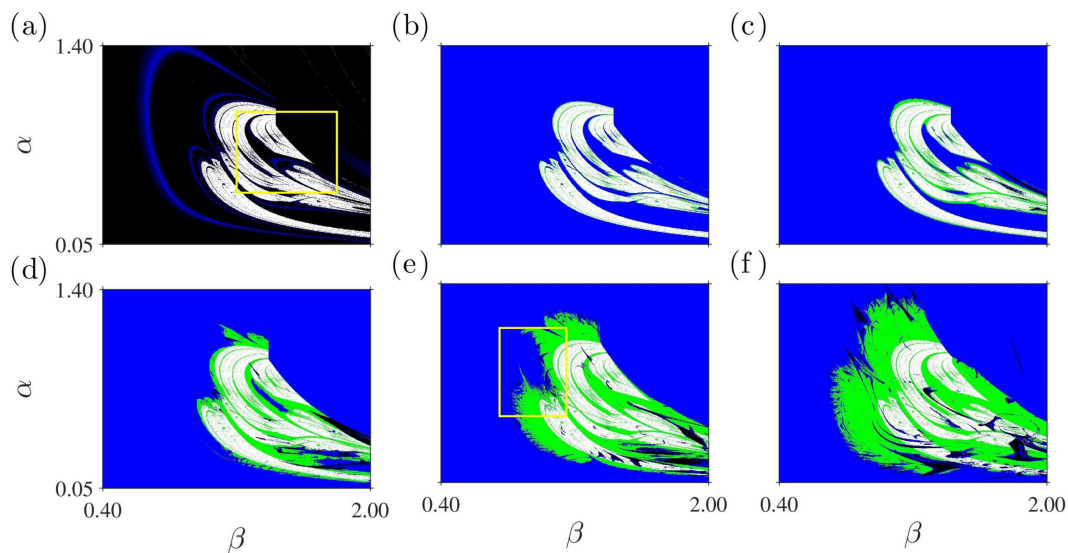


FIG. 5. Parameter plane diagrams for α vs β , showing the transformation of the periodic windows (black) at (a) $\gamma = 0.0$, under increasing perturbation: (b) $\gamma = 0.001$, (c) $\gamma = 0.005$, (d) $\gamma = 0.025$, (e) $\gamma = 0.050$, and (f) $\gamma = 0.100$. Periodic attractors are plotted in black, chaotic attractors in white, and quasiperiodic attractors in blue. The green region represents chaotic attractors previously periodic at $\gamma = 0.0$. The remaining parameters are fixed at $C = 1.2$, $L = 3.3$, and $\omega = 0.28$.

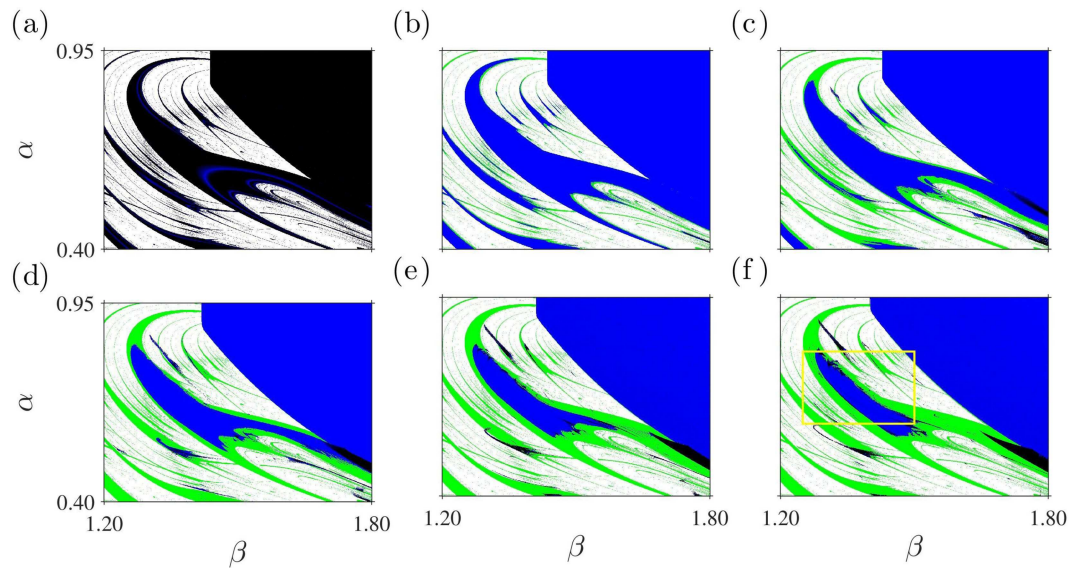


FIG. 6. Parameter plane diagrams for α vs β , illustrating the transformation of the periodic shrimp-shaped domains (black) at (a) $\gamma = 0.0$ [a magnified view of the yellow box in Fig. 5(a)], under increasing perturbation: (b) $\gamma = 0.001$, (c) $\gamma = 0.005$, (d) $\gamma = 0.010$, (e) $\gamma = 0.015$, (f) $\gamma = 0.020$. Periodic attractors are plotted in black, chaotic attractors in white, and quasiperiodic attractors in blue. The green region represents chaotic attractors previously periodic at $\gamma = 0.0$. The remaining parameters are fixed at $C = 1.2$, $L = 3.3$, and $\omega = 0.28$.

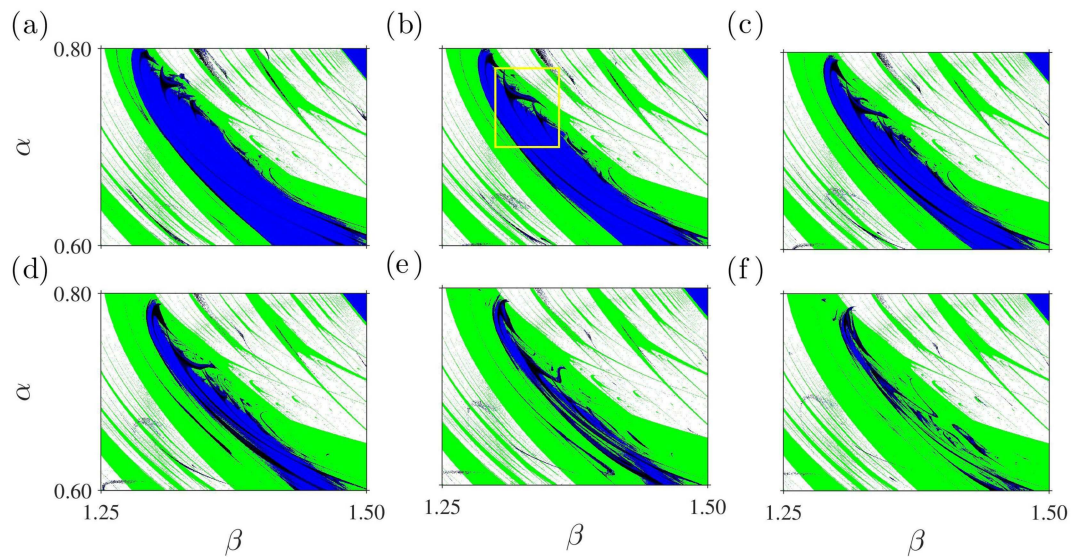


FIG. 7. Parameter plane diagrams for α vs β , illustrating the transformation of the shrimps at (a) $\gamma = 0.020$ [a magnified view of the yellow box in Fig. 6(f)], under increasing perturbation: (b) $\gamma = 0.022$, (c) $\gamma = 0.024$, (d) $\gamma = 0.026$, (e) $\gamma = 0.028$, and (f) $\gamma = 0.030$. Periodic attractors are plotted in black, chaotic attractors in white, and quasiperiodic attractors in blue. The green region represents chaotic attractors previously periodic at $\gamma = 0.0$. The remaining parameters are fixed at $C = 1.2$, $L = 3.3$, and $\omega = 0.28$.

IV. MECHANISM OF METAMORPHOSIS

In this section, we examine the mechanism behind the transformation of self-similar structures in parameter planes, with a particular focus on shrimp-shaped domains. As a preliminary step, we provide, in Figs. 8(a) and 8(b), a better picture of the self-similar pattern of the Arnold tongues. Periodic, quasiperiodic, and chaotic attractors are represented in black, red, and white, respectively. Figure 8(a) displays a magnified view of the yellow box depicted in Fig. 5(e), highlighting Arnold tongues as boundaries, while Fig. 8(b) shows a magnified region from Fig. 7(b), focusing on the tongues originating from quasiperiodic shrimp-shaped domains. In both instances, we observe the emergence of tongues in regions previously dominated by period-doubling cascades under unperturbed conditions.

Following the cyan dashed line in Fig. 8(b) associated with tongues from shrimp metamorphosis, we display, in Fig. 9(a), a bifurcation diagram for the parameter β with $\alpha = 23.909 - 33.996\beta + 12.461\beta^2$. From this diagram, we observe that the attractors linked to period-3 shrimp transformations are organized into sets of three. Therefore, the tongues consist of structures whose periods are multiples of three. Additionally, we also observe a typical pattern of periodic organization for Arnold tongues. Between windows with periods 21 and 24, we identify the major window with period 45, followed by period 69 between periods 24 and 45, and so on. For a better view of the corresponding periods, Fig. 9(b) displays

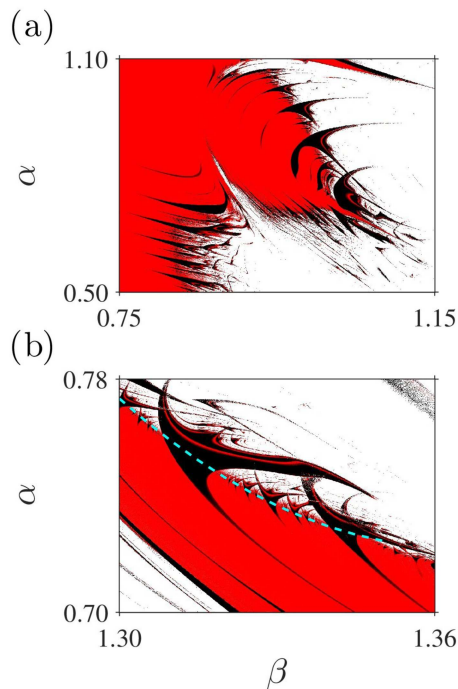


FIG. 8. Magnifications of the portion limited by yellow box of (a) Fig. 5(e) and (b) Fig. 7(b). Periodic, quasiperiodic, and chaotic attractors are depicted in black, red, and white, respectively. The red lines within the black regions correspond to period-doubling bifurcations.

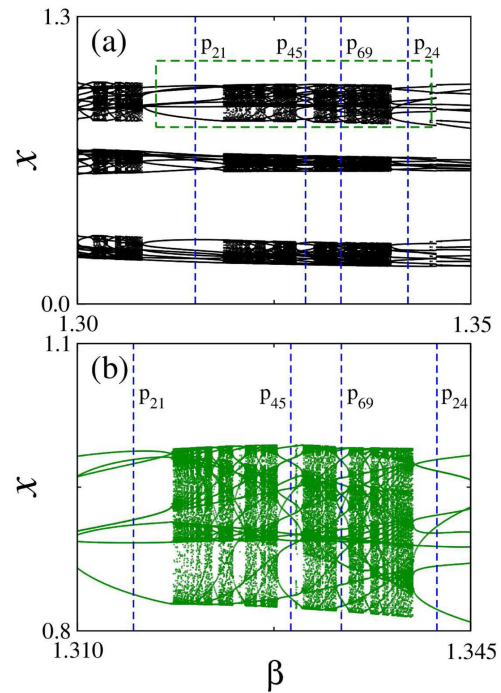


FIG. 9. (a) Bifurcation diagram following the cyan dashed line of Fig. 8(b) for the parameter β with $\alpha = 23.909 - 33.996\beta + 12.461\beta^2$. (b) Magnification of the diagram limited by the green box of (a).

a single set (one out of three) of the bifurcation diagram, from a magnification of the green dashed-line box indicated in Fig. 9(a). The attractors with periods 21, 24, 45, and 69 are represented by 7, 8, 15, and 23 lines, respectively. In the end, the organization of tongues obeys a Fibonacci-like sequence, where each window has a period equal to the sum of the periods of the two adjacent major windows.

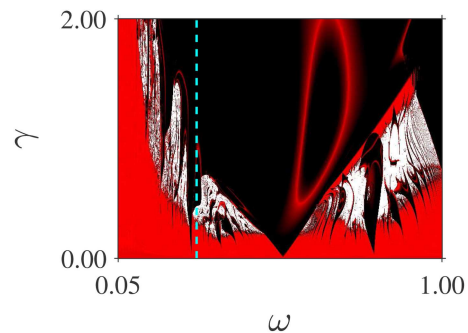


FIG. 10. Parameter plane diagram for γ vs ω , showing periodic structures (in black) organized as tongues. The parameters are fixed at $(\alpha, \beta, \gamma) = (0.7, 0.5, 0.0)$ corresponding to period-1 solution indicated as plus symbol in Fig. 3(a). Periodic, quasiperiodic, and chaotic attractors are depicted in black, red, and white, respectively. The red lines within the black regions correspond to period-doubling bifurcations.

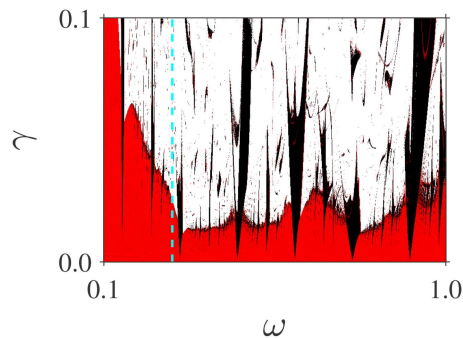


FIG. 11. Parameter plane diagram for γ vs ω , showing the appearance of tongues for the parameters $(\alpha, \beta) = (0.75, 1.30)$, selected inside of the largest shrimp region of Fig. 6(a). Periodic, quasiperiodic, and chaotic attractors are depicted in black, red, and white, respectively.

This typical phenomenon for tongues has been identified in several systems, ranging from biological²⁸ to mechanical systems.²⁹

Taking into account the mechanism behind the parameter plane transformation, as first pointed out by Furui and Takano,¹⁴ the periodically driven Muthuswamy–Chua circuit presents a Devil’s staircase, a phenomenon associated with Arnold tongues and quasiperiodic behaviors. Therefore, it is expected to identify the resonance tongues in the parameter plane diagrams corresponding to the control parameters of the perturbation. For the parameters fixed at $(\alpha, \beta, \gamma) = (0.7, 0.5, 0.0)$ corresponding to period-1 solution indicated as plus symbol in Fig. 3(a), we provide in Fig. 10 a parameter plane diagram showing the amplitude of excitation γ as a function of the frequency ω . As expected, the periodic perturbation induces the appearance of resonance tongues (in black), surrounded by quasiperiodic (in red) and chaotic (in white) regions. The red lines in the middle of black areas correspond to period-doubling bifurcations, while the cyan dashed line indicates the frequency $\omega = 0.28$ used in our simulations throughout this work.

For the control parameter values located within shrimp-shaped domains, we also observe the appearance of resonance tongues for the perturbation parameters. For instance, varying γ and ω , Fig. 11 displays the scenario of tongues for a set of parameters $(\alpha, \beta) = (0.75, 1.30)$, selected inside of the largest shrimp region of Fig. 6(a). The cyan dashed line indicates the frequency $\omega = 0.28$ used in our numerical simulations throughout this work.

Note that the property of exhibiting resonance tongues for the control parameters of periodic perturbation (γ and ω) corresponds to the essential factor for a system presenting the mechanism of self-similar domain transformation, distinguished by the presence of Arnold tongues with the shrimp metamorphosis. In other words, an originally autonomous dynamical system that develops Arnold tongues under periodic perturbation is expected to exhibit the mechanism of shrimp metamorphosis.

V. CONCLUSIONS

In this study, we numerically investigated the effect of a weak harmonic perturbation on the dynamics of the Muthuswamy–Chua circuit in two-dimensional parameter spaces. This system, composed

of a capacitor, a linear inductor, and a memristor, exhibits periodic and chaotic attractors, characterized by a period-doubling route to chaos under unperturbed conditions. By applying a weak harmonic perturbation, we initially observed the replacement of periodicity by quasiperiodicity. In fact, a weak perturbation effectively introduces a zero Lyapunov exponent into the system. In addition to converting periodicity into quasiperiodicity, perturbation also transforms chaotic attractors into chaos on torus. Increasing perturbation, we verified the emergence of periodic domains, forming Arnold tongues at the boundaries between quasiperiodic and chaotic regions. As a key finding, we also identified the metamorphosis of quasiperiodic shrimp-shaped domains into Arnold tongues. In both instances, Arnold tongues emerge in regions previously dominated by period-doubling cascades under unperturbed conditions. Moreover, these periodic tongues play an essential role in illustrating the route to chaos from quasiperiodicity, as described in the Curry–Yorke scenario.

Our findings expand the understanding of nonlinear dynamical behaviors for systems under a weak harmonic perturbation. However, further numerical investigation should be carried out to understand better the scenario involving the emergence of Arnold tongue structures. In classical nonlinear dynamics, Arnold tongues can arise in forced nonlinear oscillators where frequencies lock into rational ratios. In our investigation, we identified these mode-locking structures in the parameter plane defined by the perturbation parameters, γ and ω . In fact, Arnold tongues are typically observed for the perturbation parameters. Using the same approach, we also investigate the effect of perturbation on other systems. Initially, we characterized the systems using parameter plane diagrams defined by the perturbation parameters, and subsequently by additional parameters. For cases such as the Rössler system, we have observed that the emergence of Arnold tongues does not occur when these structures are absent for the perturbation parameters (amplitude and frequency). Therefore, the scenario presented in this study is not unique and depends on the intrinsic dynamical features of the system in which mode-locking plays a significant role.

In the end, memristors have characteristics that are useful in electronic and electrical systems. They can be used in various applications such as non-volatile memory, hardware security, and neuromorphic computing. In real circuits, the Arnold tongues can imply a predictable behavior and also lead to control strategies. Baptista and collaborators⁴⁶ showed that the Arnold tongues can exhibit robust phase synchronized states in a perturbed Chua circuit. Therefore, memristive tongues are of great importance to determine the stability or control the oscillation frequency of circuits.

ACKNOWLEDGMENTS

This study was supported by the São Paulo Research Foundation (FAPESP) under Grant Nos. 2024/05700-5 and 2024/05176-4. We are grateful for their financial support, which made this research possible. We acknowledge the 105 Group Science members for their insightful discussions (<https://www.105groupscience.com>).

AUTHOR DECLARATIONS

Conflict of Interest

The authors have no conflicts to disclose.

Author Contributions

Silvio L. T. de Souza: Conceptualization (equal); Data curation (equal); Formal analysis (equal); Investigation (equal); Methodology (equal); Validation (equal); Visualization (equal); Writing – original draft (equal); Writing – review & editing (equal). **Antonio M. Batista:** Investigation (equal); Methodology (equal); Validation (equal); Visualization (equal); Writing – review & editing (equal). **Iberê L. Caldas:** Funding acquisition (equal); Methodology (equal); Validation (equal); Visualization (equal); Writing – review & editing (equal).

DATA AVAILABILITY

The data that support the findings of this study are available from the corresponding author upon reasonable request.

REFERENCES

- L. Chua, “Memristor—The missing circuit element,” *IEEE Trans. Circuit Theory* **18**, 507–519 (1971).
- D. B. Strukov, G. S. Snider, D. R. Stewart, and R. S. Williams, “The missing memristor found,” *Nature* **453**, 80–83 (2008).
- J. J. Yang, M. D. Pickett, X. Li, D. A. A. Ohlberg, D. R. Stewart, and R. S. Williams, “Memristive switching mechanism for metal/oxide/metal nanodevices,” *Nat. Nanotechnol.* **3**, 429–433 (2008).
- T. H. Kim, E. Y. Jang, N. J. Lee, D. J. Choi, K.-J. Lee, J.-T. Jang, J.-S. Choi, S. H. Moon, and J. Cheon, “Nanoparticle assemblies as memristors,” *Nano Lett.* **9**, 2229–2233 (2009).
- M. Sparvoli, R. D. Mansano, F. O. Jorge, R. C. Rangel, G. F. B. Lenz e Silva, and J. F. D. Chubaci, “Characterization of graphene and indium tin oxynitride thin films for use as layers in resistive memories,” *Phys. Status Solidi B*, 2400575 (2025).
- J. Sun, Y. Shen, and C. Xu, “Compound synchronization of four memristor chaotic oscillator systems and secure communication,” *Chaos* **23**, 013140 (2013).
- M. D. Gregory and D. H. Werner, “Application of the memristor in reconfigurable electromagnetic devices,” *IEEE Antennas Propag. Mag.* **57**, 239–248 (2015).
- J. Zha, H. Huang, and Y. Liu, “A novel window function for memristor model with application in programming analog circuits,” *Trans. Circuits Systems II* **63**, 423–427 (2016).
- T.-H. Lee, H.-G. Hwang, J.-U. Woo, D.-H. Kim, T.-W. Kim, and S. Nahm, “Synaptic plasticity and metaplasticity of biological synapse realized in a K₂NbO₇ memristor for application to artificial synapses,” *ACS Appl. Mater. Interfaces* **10**, 25673–25682 (2018).
- M. Prezioso, F. M. Bayat, B. Hoskins, K. Likharev, and D. Strukov, “Self-adaptive spike-time-dependent plasticity of metal-oxide memristors,” *Sci. Rep.* **6**, 21331 (2016).
- B. Muthuswamy and L. O. Chua, “Simplest chaotic circuit,” *Int. J. Bifurcation Chaos* **20**, 1567–1580 (2010).
- I. A.-D. H. A. Al-Saidi and F. A. Al-Saymari, “Study of bifurcation and chaos in the Muthuswamy–Chua system,” *Chaos Solitons Fractals* **87**, 146–152 (2016).
- K. C. Iarosz, E. C. Gabrick, J. Trobia, R. R. Borges, P. R. Protachevich, R. C. Bonetti, S. L. T. de Souza, G. L. Batista, J. D. Szezech, Jr., I. L. Caldas, and A. M. Batista, “Chaotic dynamics in memristive circuits,” *Rev. Bras. Ens. Fis.* **45**, e20230116 (2023).
- S. Furui and T. Takano, “On the amplitude of external perturbation and chaos via devils’s staircase—Stability of attractors,” *Int. J. Bifurcation Chaos* **25**, 1550145 (2015).
- X. Xu, M. Wiercigroch, and M. P. Cartmell, “Rotating orbits of a parametrically-excited pendulum,” *Chaos Solitons Fractals* **23**, 1537–1548 (2005).
- S. L. T. de Souza and I. L. Caldas, “Calculation of Lyapunov exponents in systems with impacts,” *Chaos Solitons Fractals* **19**, 569–579 (2004).
- S. L. T. de Souza, I. L. Caldas, and R. L. Viana, “Multistability and self-similarity in the parameter-space of a vibro-impact system,” *Math. Probl. Eng.* **2009**, 290356.
- J. Slipantschuk, E. Ullner, M. S. Baptista, M. Zeineddine, and M. Thiel, “Abundance of stable periodic behavior in a red grouse population model with delay: A consequence of homoclinicity,” *Chaos* **20**, 045117 (2010).
- M. Hossain, S. Garai, S. Jafari, and N. Pal, “Bifurcation, chaos, multistability, and organized structures in a predator–prey model with vigilance,” *Chaos* **32**, 063139 (2022).
- R. Rajini and B. Ghosh, Arnold tongues, shrimp structures, multistability, and ecological paradoxes in a discrete-time predator–prey system,” *Chaos* **34**, 123103 (2024).
- M. S. Bittencourt, E. L. Brugnago, Z. O. Guimarães-Filho, I. L. Caldas, and A. S. Reis, “How a responsive reproduction factor is determinant in a prey–predator dynamics: A numerical and analytical study in a discrete-time model,” *Chaos* **35**, 013154 (2025).
- H. A. Albuquerque, R. M. Rubinger, and P. C. Rech, “Self-similar structures in a 2D parameter-space of an inductorless Chua’s circuit,” *Phys. Lett. A* **372**, 4793–4798 (2008).
- A. A. C. Recco, J. C. Sagás, and P. C. Rech, “Multistability, period-adding, and fractality in a plasma oscillator,” *Phys. Plasmas* **30**, 112301 (2023).
- A. A. Alvarez, E. L. Brugnago, and I. L. Caldas, “Routes to chaos and bistability in the Rypdal model with a parametric disturbance,” *Chaos Solitons Fractals* **186**, 115246 (2024).
- J. A. Gallas, “Dissecting shrimps: Results for some one-dimensional physical models,” *Physica A* **202**, 196–223 (1994).
- K. Ullmann and I. L. Caldas, “Transitions in the parameter space of a periodically forced dissipative system,” *Chaos Solitons Fractals* **7**, 1913–1921 (1996).
- M. S. Baptista and I. L. Caldas, “Dynamics of the kicked logistic map,” *Chaos Solitons Fractals* **7**, 325–336 (1996).
- S. L. T. de Souza, A. A. Lima, I. L. Caldas, R. O. Medrano-T., and Z. O. Guimarães-Filho, “Self-similarities of periodic structures for a discrete model of a two-gene system,” *Phys. Lett. A* **376**, 1290–1294 (2012).
- S. L. T. de Souza, A. M. Batista, M. S. Baptista, I. L. Caldas, and J. M. Balthazar, “Characterization in bi-parameter space of a non-ideal oscillator,” *Physica A* **466**, 224–231 (2017).
- M. Hansen, D. R. da Costa, D. F. M. Oliveira, and E. D. Leonel, “Statistical properties for a dissipative model of relativistic particles in a wave packet: A parameter space investigation,” *Appl. Math. Comput.* **238**, 387–392 (2014).
- D. R. da Costa, M. Hansen, G. Guarise, R. O. Medrano-T., and E. D. Leonel, “The role of extreme orbits in the global organization of periodic regions in parameter space for one dimensional maps,” *Phys. Lett. A* **380**, 1610–1614 (2016).
- R. Varga, K. Klapcsik, and F. Hegedüs, “Route to shrimps: Dissipation driven formation of shrimp-shaped domains,” *Chaos Solitons Fractals* **130**, 109424 (2020).
- N. V. Stankevich, N. A. Shchegoleva, I. R. Sataev, and A. P. Kuznetsov, “Three-dimensional torus breakdown and chaos with two zero Lyapunov exponents in coupled radio-physical generators,” *J. Comput. Nonlinear Dyn.* **15**, 111001 (2020).
- N. C. Pati, “Spiral organization of quasi-periodic shrimp-shaped domains in a discrete predator–prey system,” *Chaos* **34**, 083126 (2024).
- N. C. Pati, P. Datta, and B. Ghosh, “Exploring quasi-periodic shrimps in the parameter space of a discrete-time food chain model,” *Chaos* **35**, 023101 (2025).
- S. L. T. de Souza, A. M. Batista, R. O. Medrano-T., and I. L. Caldas, “Quasiperiodic shrimp-shaped domains in intrinsically coupled oscillators,” *Chaos* **34**, 123146 (2024).
- G. Benettin, L. Galgani, A. Giorgilli, and J.-M. Strelcyn, “Lyapunov characteristic exponents for smooth dynamical systems and for Hamiltonian systems; a method for computing all of them. Part 1: Theory,” *Meccanica* **15**, 9–20 (1980).
- A. Wolf, J. B. Swift, H. L. Swinney, and J. A. Vastano, “Determining Lyapunov exponents from a time series,” *Physica D* **16**, 285–317 (1985).
- J. H. Curry and J. A. Yorke, “A transition from Hopf bifurcation to chaos: Computer experiments with maps on \mathbb{R}^2 ,” in *The Structure of Attractors in Dynamical Systems* (Springer, 1978), pp. 48–66.
- C. Letellier, V. Messager, and R. Gilmore, “From quasiperiodicity to toroidal chaos: Analogy between the Curry–Yorke map and the van der Pol system,” *Phys. Rev. E* **77**, 046203 (2008).

⁴¹M. Mugnaine, A. M. Batista, I. L. Caldas, J. D. Szezech, Jr., R. E. de Carvalho, and R. L. Viana, "Curry–Yorke route to shearless attractors and coexistence of attractors in dissipative nontwist systems," *Chaos* **31**, 023125 (2021).

⁴²U. Feudel, J. Kurths, and A. S. Pikovsky, "Strange non-chaotic attractor in a quasiperiodically forced circle map," *Physica D* **88**, 176–186 (1995).

⁴³O. Sosnovtseva, U. Feudel, J. Kurths, and A. Pikovsky, "Multiband strange non-chaotic attractors in quasiperiodically forced systems," *Phys. Lett. A* **218**, 255–267 (1996).

⁴⁴S. Kuznetsov, U. Feudel, and A. Pikovsky, "Renormalization group for scaling at the torus-doubling terminal point," *Phys. Rev. E* **57**, 1585–1590 (1998).

⁴⁵T. Mitsui, S. Uenohara, T. Morie, Y. Horio, and K. Aihara, "Torus-doubling process via strange nonchaotic attractors," *Phys. Lett. A* **376**, 1907–1914 (2012).

⁴⁶M. S. Baptista, T. P. Silva, J. C. Sartorelli, I. L. Caldas, and E. Rosa, "Phase synchronization in the perturbed Chua circuit," *Phys. Rev. E* **67**, 056212 (2003).